Structural Characterization of Worm Images Using Trace Transform and Backpropagation Neural Network

Chandan Chakraborty

School of Medical Science & Technology
Indian Institute of Technology Kharagpur, India
chandanc@smst.iitkgp.ernet.in

Abstract

Various diseases caused by pathogenic parasites and fungi may be characterized by shape based structures. No significant attempt has been made so far to categorize such parasites by their shape properties, which can make the task of information retrieval much easier than annotating all of them separately. Here we present an automatic classification system which can retrieve the parasite or fungi's information from the database using shape based information. To reduce time complexity of the information retrieval parasites having more or less identical shapes are clustered in the same group. A set of shape descriptors, generated by trace transform has been used to characterize structure of worms. Backpropagation neural network is trained, which leads to 85.71% accuracy of classification using statistically significant shape features.

Keywords: *Worm images, shape descriptors, Hu moments, Trace transform, Back propagation neural network*

1. Introduction

Retrieving information about images from large image databases in accordance to users' interests has been an active and fast advancing research area since 1990s. During the past decade, remarkable progress has been made in both theoretical research as well as system development. Initial attempts in this direction were based on the search of the text annotated with the images [1, 2]. Such systems however, provide only limited accuracy since in practice; many relevant images come with incorrect caption, or with imprecise information. Most of the text based image retrieval requires manual annotation of images which is a tedious task in case of retrieval from large image database. These issues are usually raised in diverse applications of computer vision.

In order to resolve these issues, the proposed work aims at introducing a new application based on pattern shape detection. Here we present an interesting application of classification of various worms, parasites and fungi by their shape properties. This system is of vital importance when one wants to retrieve structural information of a parasite image without having much knowledge about its associated text. A major advantage of such a system is that a user, without having much knowledge of worm, parasite or fungi, may retrieve the detail information as well as a set of similar images of any parasite, fungi or worm at any stage.

Here we present such a system using 150 image patterns with 30 samples in each five classes of worm. Each class represents a different parasite having its own characteristic shape features. In order to segment parasites' boundaries from complex and noisy images,

histogram based thresholding is performed. Afterwards, various features are extracted from each segmented object. In this work, standard shape descriptors like convexity, compactness and eccentricity etc, Hu moments and Trace transform based descriptors are studied for description and recognition of worm shapes. Next, significance of each descriptor is evaluated statistically, which gives a set of significant discriminating features to retrieve images. In this study, these significant features lead to 85.71% accuracy of the backpropagation neural network [3] for classification.

Section 2 gives information about the various worms, parasites and fungi which are used to study their shape properties. In Section 3 various shape based descriptors have been studied for worm image retrieval and these are statistically analyzed to show their significance. Section 4 describes backpropagation neural network for classification of a query worm image into the most likely worm class. Then the results are shown and discussed in Section 5 and some concluding remarks are reported in Section 6.

2. Materials

In this research we have aimed at creating a database of five classes of most common worm that are responsible for the disorder in human organs. Our database contains 150 worm images belonging to five classes. Each class represents a different parasite having its own characteristic shape properties. 30 shapes of each type of parasite have been studied. A brief description for each parasite class is given below.

(a) ***Balatidium coli*** (http://www.soton.ac.uk) - It is the largest protozoan parasite (see Figure 1. A1) of humans. It has strains that will adapt to other species and cause disease. It also produces proteolytic enzymes that break down and digest the intestinal epithelium. The liver or lung can be infected. They are oblong, spheroid, or slender. They are 30-50 microns long and 20-120 microns wide.

(b) ***Fasciolopsis buski*** (http://www.doctorfungus.org) - It is the largest intestinal fluke (see Figure 1. B1). The adult measures 2-7.5 cm by 0.8-2 cm by 0.5-3 mm and lives in the small intestine and occasionally in the colon and the pylorus attached to the mucosa. Light infections are usually asymptomatic, but heavily infected individuals may present abdominal pain, diarrhea, malabsorption, toxaemia.

(c) ***Aspergillus niger*** (http://parasite.natur.cuni.cz) - It is a fungus and one of the most common species of the genus Aspergillus, (see Figure 1. C1). It causes a disease called black mold on certain fruits and vegetables such as grapes, onions, and peanuts, and is a common contaminant of food. This is the third most common species associated with invasive pulmonary aspergillosis. It is also often a causative agent of aspergilloma and is the most frequently encountered agent of otomycosis. *Aspergillus* is especially prevalent in the air. Hyphae are septate and hyaline. Conidial heads are radiate initially, splitting into columns at maturity. Conidiophores are long (400-3000 μm), smooth, and hyaline, becoming darker at the apex and terminating in a globose

vesicle (30-75 μm in diameter). The slides were stained using Lactophenol cotton blue.

(d) ***Tape worm*** **(**www.doctorsecrets.com) **-** Cestoda is the class of parasitic flatworms, commonly called tapeworms (see Figure 1. D1), which live in the digestive tract of vertebrates as adults and often in the bodies of various animals as juveniles. The people that have been infected by this tapeworm have described the following symptoms: abdominal discomfort and pain, cramp, colic, flatulence, diarrhea, tiredness, malabsorption, vitamin deficiency, megaloblastic anemia, weight loss. Furthermore, through self-infection of Taenia Solium (the pork tapeworm) there has been in the past a serious life threatening infections of taeniais which may make the chances of neurocysticercosis go higher.

(e) ***Ascaris*** (www.drnatura.com/parasites.php) **-** Ascaris lumbricoides (see Figure 1. E1) evolved with humans, and it lives in the intestines of millions of people. Large and active, it has inspired many tales and considerable folklore. Ascaris lumbricoides is otherwise known as the large intestinal roundworm of humans. Ascaris lumbricoides worms have a reputation for wandering, and often do so if the body they are in—the host—is ill or taking certain medications and may cause illness in the host. Adult roundworms sometimes spontaneously exit the host through the anus, mouth, or nose. Females can be well over a foot long; males are smaller.

3. Shape-based Worm Image Retrieval

The overall architecture of the proposed system is shown in Figure 2. Initially, the whole image database having worm, fungi and parasite is considered, as input to the system, to extract various shape descriptors. Next, these descriptors are statistically analyzed using F-test and *p*-value for their significance study. Afterwards, classification of a query image is performed using backpropagation neural network to retrieve the most likely labeled worm class.

A1 A2

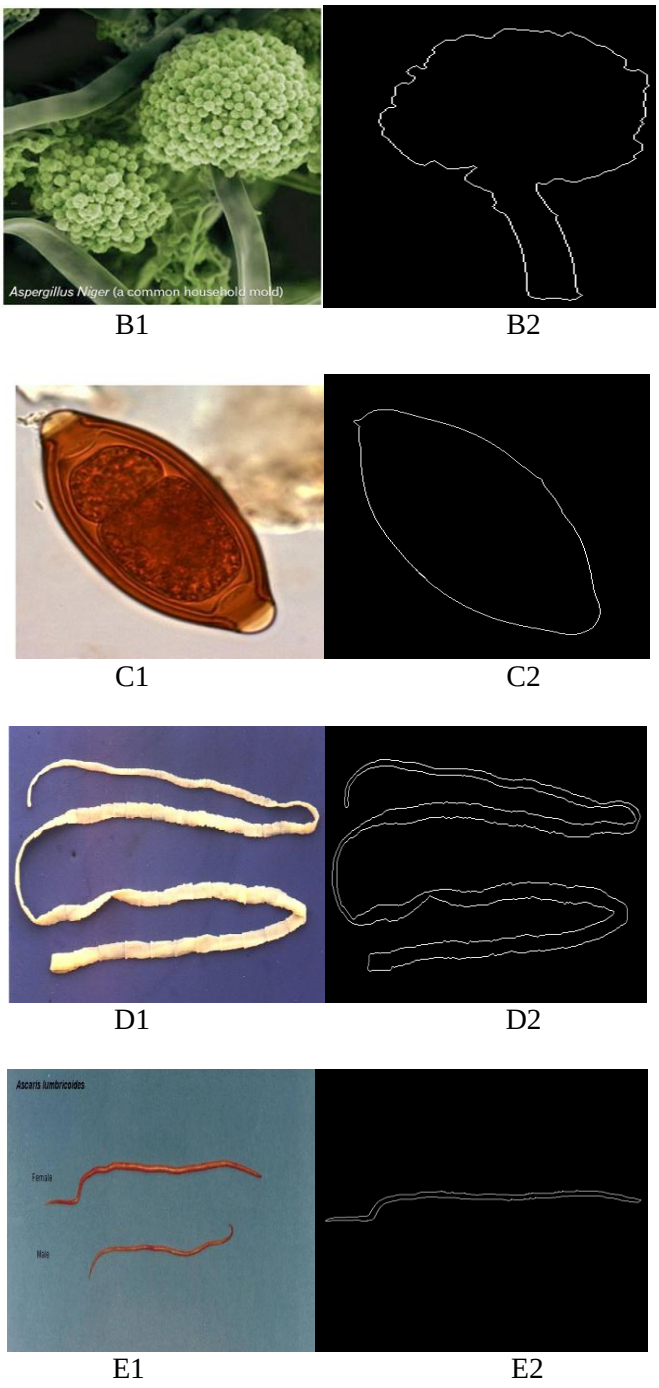

Figure 1. (A1) Balatidium Coli and (A2) its segmented boundary, (B1) Aspergillus niger and (B2) its segmented boundary, (C1) Fascilopsis buski and (C2) its segmented boundary, (D1) Tape worm and (D2) its segmented boundary, (E1) Ascaris and (D2) its Segmented Boundary

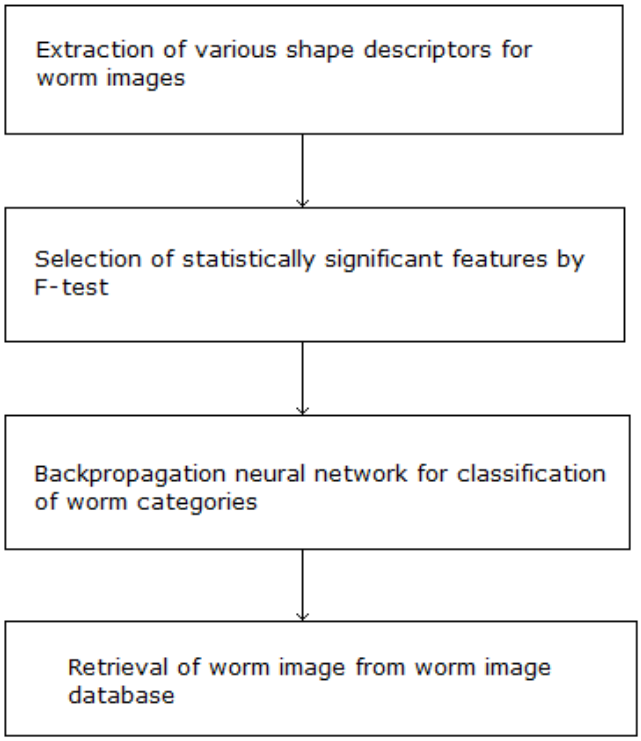

Figure 2. Proposed System for Shape Based Image Retrieval

3.1 Image segmentation

Image segmentation is the fundamental step for classification of images. First step is to convert the grayscale image into binary image by histogram based thresholding using Otsu method [4]. Otsu method is based upon minimizing within class variance or maximizing the between class variance. Threshold value (say T) depends only on the difference between the means of the two clusters, thus avoids calculating differences between individual intensities and the cluster means. If *'μ_B'* and *'μ_O'* denote the means of two classes respectively, and *'n_B'* and *'n_O'* indicate no. of pixels in each cluster then between class variance can be calculated by

$$\sigma^2_{between}(T) = n_B(T)n_o(T)(\mu_B - \mu_O)^2 \quad (1)$$

Sobel edge detection is applied to find the edge after performing morphological operations on the segmented image. The output boundary from Sobel edge detection is not properly connected so it is connected by 8-neighbourhood connectivity [5, 6]. These connected boundaries have been labeled by connected component labeling to distinguish the object boundary and other unwanted boundaries. The label having maximum no. of pixels shows the desired object boundary.

Each worm is geometrically described using various shape descriptors. These descriptors are expected to be lesser variant within each class. Some of the shapes, belonging to five classes, from the image database of 150 worm, parasite and fungi are shown in Figure 3.

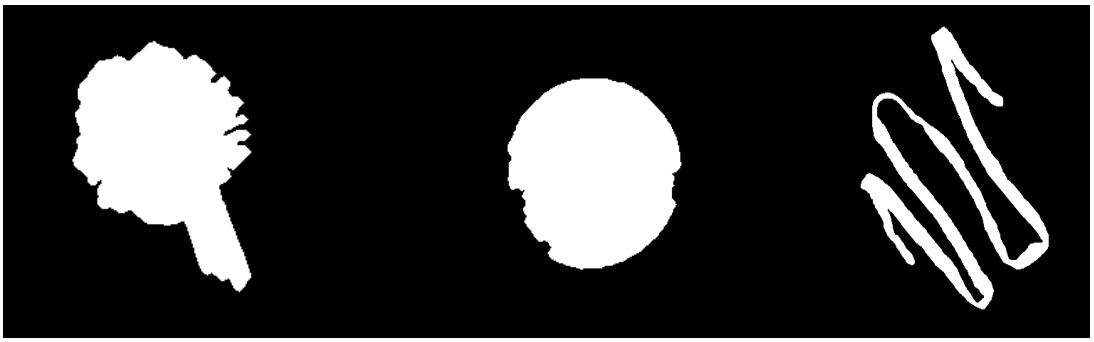

(1) (2) (3)

(4) (5) (6)

(7) (8) (9)

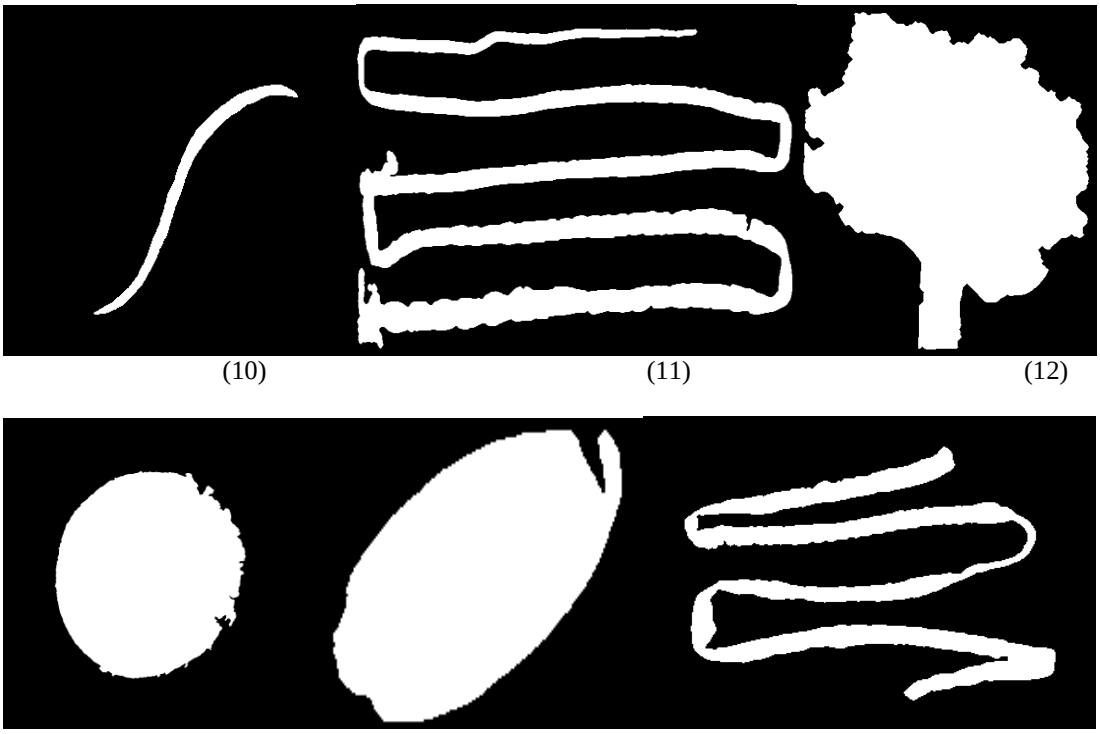

Figure 3. Fifteen Extracted Shapes of the Worms, Fungi and Parasites

3.2.1 Convexity

Convexity is one of the very essential properties of shapes. Studies have been done to measure of convexity including fuzzy convexity measure [7], approximate convexity measures [9], Multi-Scale Auto convolution (MSA) etc. Out of these here MSA [8] has been used to measure the convexity. This measure is advantageous since it leads to higher accuracy of convexity with less computational complexity. Mathematically, the formula to compute convexity using MSA method, is given by

$$F(\frac{1}{2},\frac{1}{2}) = \frac{1}{N_1 N_2}\frac{1}{\mathcal{F}(0)^2}\sum_{i=0}^{N_1 N_2 - 1}\mathcal{F}^*(w_i)\mathcal{F}(\frac{1}{2}w_i)^2 \tag{2}$$

where F(.) is the Fourier transform of the image f having $N_1 \times N_2$ pixels. Convexity is close to 1 for perfectly convex shapes such as ellipse and circle (see table 1). So such shape can be discriminated easily by the convexity descriptor. Balatidium coli being almost circular in shape and Fascilopsis buski being somewhat elliptical in shape have high convexity while the convexity of a tape worm is less. Moreover, convexity is also rotation, scaling and translation invariant. Hence its geometrical distortions or orientations do not affect its value.

Table 1. Convexity Values of 30 Worms in Class 5 and its Mean & Variance

Serial Sample No. (class 5)	Convexity	Mean convexity	Variance
E1	0.5176	0.4698	0.0142
E2	0.5176		
E3	0.6385		
E4	0.6397		
E5	0.5048		
E6	0.5087		
E7	0.5168		
E8	0.5327		
E9	0.5323		
E10	0.5124		
E11	0.3506		
E12	0.3408		
E13	0.3476		
E14	0.5623		
E15	0.5796		
E16	0.337		
E17	0.3546		
E18	0.3382		
E19	0.2827		
E20	0.291		
E21	0.5868		
E22	0.6787		
E23	0.5404		
E24	0.5419		
E25	0.5584		
E26	0.3641		
E27	0.3538		
E28	0.5911		
E29	0.3685		
E30	0.3044		

3.2.2 Eccentricity

Eccentricity is well known shape property for any contour. One can use covariance matrix of all the X and Y coordinates of pixel points in a shape to calculate the eccentricity. Eigen values of the covariance matrix are used to obtain the eccentricity of the shape. As eigen vectors give the information about major and minor axis of shape. Hence, it is calculated by

$$Eccentricity = \frac{Length\ of\ Minor\ Axis}{Length\ of\ Major\ Axis} \tag{3}$$

Table 2. Eccentricity Values of 30 Worms in Class 3 and its Mean & Variance

Serial Sample No. (class 3)	Eccentricity	Mean Eccentricity	Variance
C1	0.8452	0.7912	0.0119
C2	0.8887		
C3	0.8746		
C4	0.9182		
C5	0.7579		
C6	0.9177		
C7	0.7214		
C8	0.7336		
C9	0.5378		
C10	0.8431		
C11	0.8076		
C12	0.8887		
C13	0.887		
C14	0.8731		
C15	0.8745		
C16	0.919		
C17	0.9194		
C18	0.7619		
C19	0.7604		
C20	0.726		
C21	0.7346		
C22	0.7299		
C23	0.7285		
C24	0.5377		
C25	0.5405		
C26	0.8416		
C27	0.8288		
C28	0.8064		
C29	0.8075		
C30	0.7248		

Eccentricity is 1 for circle and less than 1 for ellipse. So this feature gives more information to distinguish circle from ellipse which may not be got from convexity (see Table 2).

3.2.3 Compactness

Compactness is a dimensionless quantity, which is also insensitive to uniform scale changes. It is minimal for a circular shaped region (see table 3). By definition, it is computed by

$$Compactness = \frac{Area \quad of \quad object}{(Perimeter)^2} \tag{4}$$

Table 3. Compactness Values of 30 Worms in Class 2 and its Mean & Variance

Serial Sample No. (Class 2)	Compactness	Mean Compactness	Variance
B1	0.0384	0.0319	8.1335e-005
B2	0.0356		
B3	0.0421		
B4	0.0281		
B5	0.0403		
B6	0.027		
B7	0.0349		
B8	0.0387		
B9	0.0337		
B10	0.0236		
B11	0.024		
B12	0.0376		
B13	0.0284		
B14	0.014		
B15	0.028		
B16	0.0395		
B17	0.0336		
B18	0.0366		
B19	0.0442		
B20	0.0444		
B21	0.0234		
B22	0.0426		
B23	0.0281		
B24	0.0435		
B25	0.0271		
B26	0.0319		
B27	0.016		
B28	0.0183		
B29	0.0395		
B30	0.0153		

This descriptor is also rotation, scaling and translation invariant like others two stated above.

3.2.4 Trace Transform

Trace transform [10], generalization of Radon transform, consists of tracing an image with straight lines along which certain functional of the image function are calculated. Radon transform of an image is the value of the integral of the image computed along the tracing line which is characterized by two parameters: (a) its distance *'p'* from the center of the axes and (b) the orientation *'φ'* which is the angle between the normal to the line and the reference axis (Figure 4). Trace transform calculates functional T over parameter *t* along the line, which is not necessarily the integral. Different functional may be used to produce different trace transforms from the same image. The more classes of objects one has to identify, the more features are needed, particularly when the objects are subject to complex transformations under which their appearance may change significantly. The triple feature method allows the construction of many features easily.

Invariant feature construction

Let us consider an image F1, which may be considered to be a set of tracing lines. Each tracing line (*t*) being parameterized by (*p*, *φ*) and hence the image F1 can be denoted by F1 (*t*, *p*, *φ*). Again consider another image F2 which is a scaled, rotated and translated version of F1. F2 can be obtained from F1 by rotating F1 with an angle θ in the counter-clock wise direction, scaling by parameter '*v*' and translating it by vector ($S_o \cos\psi_o$, $S_o \sin\psi_o$). Here S_o indicates distance between centers of F1 and F2; ψ_o denotes the angle between reference axis and line joining two centers of these images.

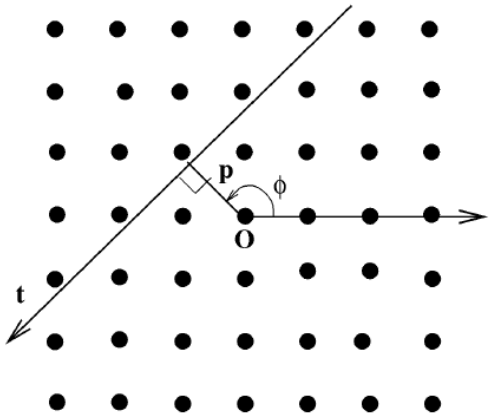

Figure 4. Tracing line with Parameters *t*, *p* and *φ*

A trace functional T is the invariant functional that is applied to the image for eliminating variable '*t'*. Similarly diametrical (P) and circus (Φ) functional may be defined as those which when applied to the result obtained after applying trace and diametrical functional eliminates variables *'p'* and *'φ'* respectively. *'Φ'*, *''P'* and T can be any one of the invariant functional as shown in Table 4. Hence

$$\Pi (F1) = \Phi (P (T (F1 (t, p,\varphi)))). \quad (5)$$

It can be shown easily that

$$\Pi (F2) = \Pi (F1) \times \nu^{\lambda_\Phi(\kappa_T\lambda_P+\kappa_P)} \quad (6)$$

where κ and λ are the properties of the functional as explained henceforth. Suppose a functional $\Xi(\xi(x))$ is used. Then, κ is defined as, $\Xi(\xi(ax)) = \Xi(\xi(x))\times a^{\kappa}$. And λ is defined as $\Xi(c\xi(x)) = \Xi(\xi(x))\times c^{\lambda}$. For the sake of simplicity, let us take $\omega = -\lambda_\Phi(\kappa_T\lambda_P+\kappa_P)$, and therefore $\Pi(F2) = \Pi(F1)\times \nu^{-\omega}$. Now the equation of the normal to the trace functional is given as

$$\Pi_{norm}(F1)=\text{sign}(\Pi(F1))\times|\Pi(F1)|^{1/\omega} \quad (7)$$

Therefore from equation (6) and (7), $\Pi_{norm}(F2)= \Pi_{norm}(F1)\times\nu^{-1}$

From equation (5), (6) and (7) it can be seen that Π_{norm} is unique to every ordered triplet of trace, diametrical and circus functionals and for the sake of convenience will be denoted as (T,P,Φ) hereafter. Ratio of two triple features is thus invariant to scaling, rotation and translation. $\Pi_i = (T_1,P_1,\Phi_1)/(T_2,P_2,\Phi_2)$ indicates the ratio of normalized triple feature triplet (T_1,P_1,Φ_1) to (T_2,P_2,Φ_2) applied in order whose normalization process is as explained above.

Table 4. Invariant Functionals with its Properties

Invariant Functional			
No.	Functional	κ	λ
IF_1	$\int \xi(t)\, dt$	-1	1
IF_2	$(\int \lvert\xi(t)\rvert^{q}\, dt)^{r}$	-r	q
IF_3	$\int \lvert\xi(t)'\rvert\, dt$	0	1
IF_4	$\max(\xi(t))$	0	1
IF_5	$IF_4 - \min(\xi(t))$	0	1

New functionals may be created from these five functionals (see Table 4). The properties of these newer ones are shown in the following table.

Table 5. Properties of New Functionals

New Functionals			
No	Functional	κ	λ
1	$\Xi_1\Xi_2$	$\kappa_{\Xi1}+\kappa_{\Xi2}$	$\lambda_{\Xi1}+\lambda_{\Xi2}$
2	$(\Xi)^{q}$	$q\kappa_\Xi$	$q\lambda_\Xi$
3	Ξ_1/Ξ_2	$\kappa_{\Xi1}-\kappa_{\Xi2}$	$\lambda_{\Xi1}-\lambda_{\Xi2}$

The various trace descriptors used in our current work are:

$$\Pi_1=\frac{(\mathrm{IF}_1,\mathrm{IF}_{2a},\mathrm{IF}_5)}{(IF_1,IF_5,IF_5)},\quad \Pi_2=\frac{(\mathrm{IF}_1,\mathrm{IF}_{2a},\mathrm{IF}_4)}{(IF_1,IF_1,IF_1)},\quad \Pi_3=\frac{(\mathrm{IF}_1,\mathrm{IF}_{2a},\mathrm{IF}_4)}{(IF_1,IF_3,IF_3)},\quad \Pi_4=\frac{(\mathrm{IF}_1,\mathrm{IF}_{2a},\mathrm{IF}_4)}{(IF_1,IF_5,IF_5)},$$

$$\Pi_5=\frac{(\mathrm{IF}_1,\mathrm{IF}_3,\mathrm{IF}_1)}{(IF_1,IF_1,IF_1)},\quad \Pi_6=\frac{(\mathrm{IF}_1,\mathrm{IF}_3,\mathrm{IF}_1)}{(IF_1,IF_{2a},IF_3)},\quad \Pi_7=\frac{(\mathrm{IF}_1,\mathrm{IF}_3,\mathrm{IF}_1)}{(IF_1,IF_5,IF_5)},\quad \Pi_8=\frac{(\mathrm{IF}_1,\mathrm{IF}_4,\mathrm{IF}_5)}{(IF_1,IF_1,IF_1)},$$

$$\Pi_9=\frac{(\mathrm{IF}_1,\mathrm{IF}_4,\mathrm{IF}_5)}{(IF_1,IF_{2a},IF_4)},\quad \Pi_{10}=\frac{(\mathrm{IF}_1,\mathrm{IF}_5,\mathrm{IF}_3)}{(IF_1,IF_1,IF_1)},\quad \Pi_{11}=\frac{(\mathrm{IF}_1,\mathrm{IF}_5,\mathrm{IF}_3)}{(IF_1,IF_{2a},IF_4)}.$$

Here, IF_{2a} means IF_2 for $q = 2$ and $r = 0.5$.

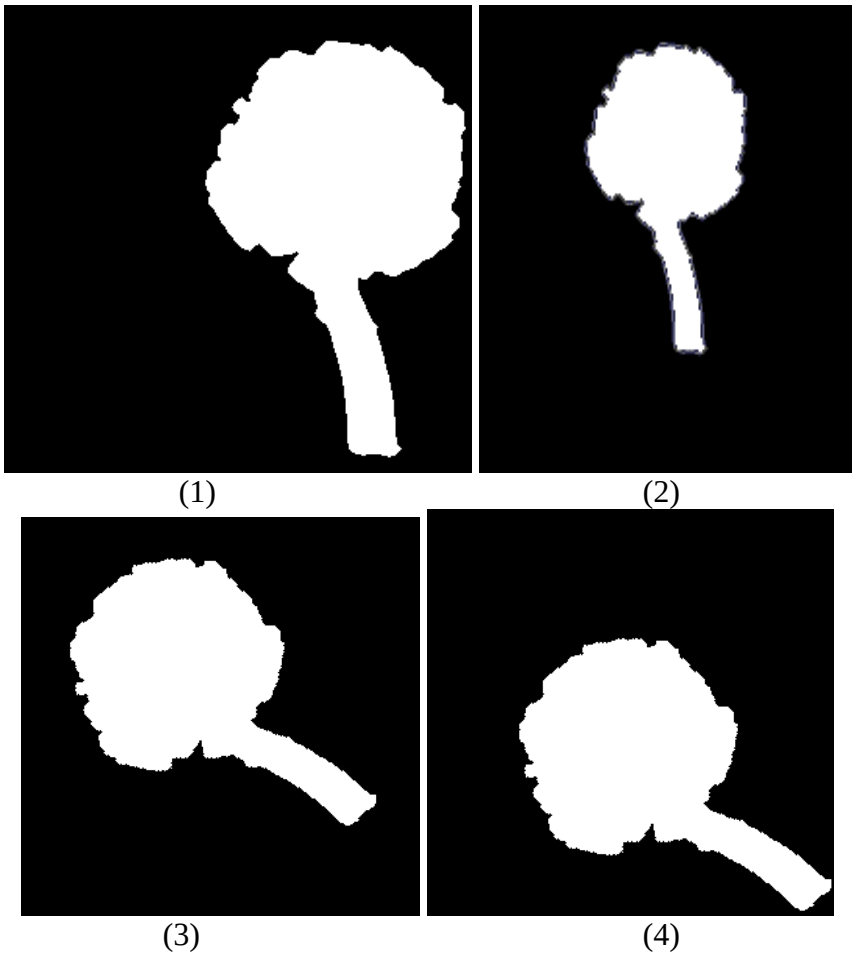

Figure 5. Scaled, rotated and translated shapes extracted from the same Aspergillus niger

Table 6. Invariant Nature of Trace Descriptor for Figure 5

Ratio of triple features $\Pi_{norm\_1}/\Pi_{norm\_2}$ of worms			
Serial Number	Π_4	Serial Number	Π_8
Fig. 5 (1)	0.2305	Fig. 5 (1)	0.8476
Fig. 5 (2)	0.2269	Fig. 5 (2)	0.8593
Fig. 5 (3)	0.2348	Fig. 5 (3)	0.8348
Fig. 5 (4)	0.2347	Fig. 5 (4)	0.8352

The use of trace descriptors for the classification of rotated, translated and scaled versions of worms were initially tested using 3 images of each class and 2 trace descriptors were used to plot for the same.

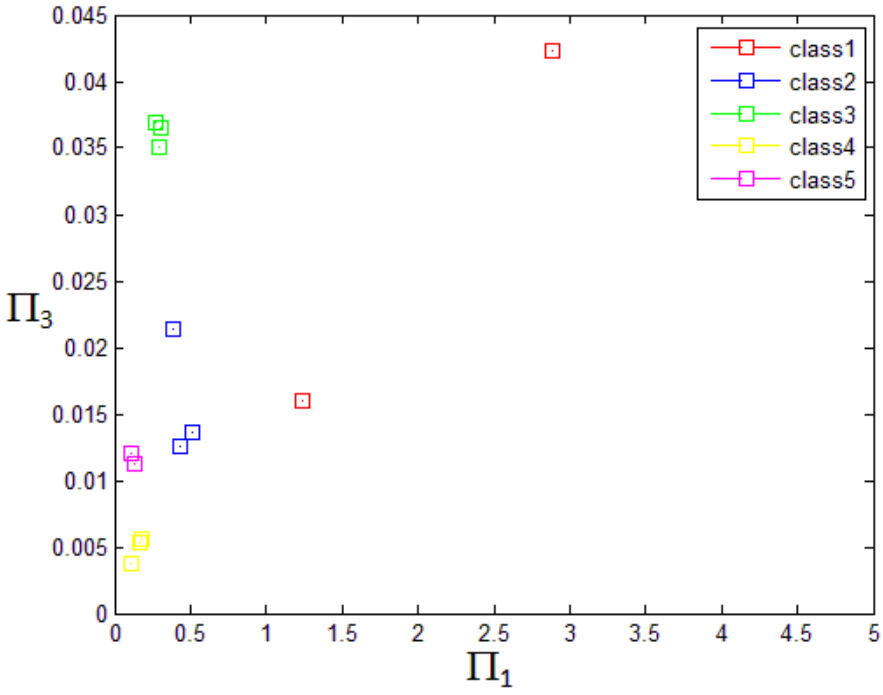

Figure 6. Clustering of Five Classes using Two Trace Descriptors

In the graph above, a pair of ratio features Π_1 vs Π_3 is plotted to make clearer the fact that descriptors of trace transform indeed helps in clustering.

Table 7. Π5 Values of 30 Worms in Class 1 and its Mean & Variance

Samples (class 1)	Π_5	Mean Π_5	Variance
A1	474.2444	486.8893	217.4889
A2	483.1781		
A3	467.6214		
A4	469.8017		
A5	482.4055		
A6	470.3426		
A7	500.8823		
A8	511.5001		
A9	498.4697		
A10	500.6473		
A11	487.4468		
A12	473.9208		
A13	471.6909		
A14	473.6079		
A15	477.9093		
A16	468.6064		
A17	467.7787		
A18	481.1181		
A19	481.3572		
A20	498.4645		
A21	501.287		
A22	516.363		
A23	518.0174		
A24	492.971		
A25	491.88		
A26	488.3434		
A27	486.3717		
A28	485.9281		
A29	479.4223		
A30	505.1015		

These features may not have any physical meaning according to human perception, but they have the right mathematical properties which would allow one to distinguish objects under a certain group of transformations. The features are invariant to geometrical distortions and hence have been used for clustering. The number of descriptors used is large to improve the efficiency of the overall system. As the number of classes to be clustered is usually large in an actual image retrieval system, more number of descriptors can be readily used using trace transform and hence a very robust system can be made. The features that are computed using trace transform are not necessarily independent.

3.2.5 Hu's Invariant Moments

The non-orthogonal centralized moments are translation invariant and can be normalized with respect to changes in scale. In 1962, Hu [11] introduced two different methods for producing rotation invariant moments. The first method called as principal axes, enables to break down when images do not have unique principal axes. Such images are described as being rotationally symmetric. The second one is the method of absolute moment invariants. Hu derived these expressions from algebraic invariants applied to the moment generating function under a rotation transformation. These consist of groups of nonlinear centralized moment expressions. The result is a set of absolute orthogonal (i.e. rotation) moment invariants, which can be used for scale, position, and rotation invariant pattern identification. These were used in a simple pattern recognition experiment to successfully identify various types of characters. These are computed from normalized centralized moments up to order three and are shown below:

$$I_1 = \eta_{20}+\eta_{02}$$

$$I_2 = (\eta_{20}-\eta_{02})^2+4\,\eta_{11}^2$$

$$I_3 = (\eta_{30}-3\,\eta_{12})^2+(3\eta_{21}-\eta_{03})^2$$

$$I_4 = (\eta_{30}+\eta_{12})^2+(\eta_{21}+\eta_{03})^2$$

$$I_5 = (\eta_{30}-3\,\eta_{12})(\eta_{30}+\eta_{12})[(\eta_{30}+\eta_{12})^2-3(3\eta_{21}-\eta_{03})^2] + (3\eta_{21}-\eta_{03})(\eta_{21}+\eta_{03})[3(\eta_{30}+\eta_{12})^2 -(3\eta_{21}-\eta_{03})^2]$$

$$I_6 = (\eta_{20}-\eta_{02})[(\eta_{30}+\eta_{12})^2-(3\eta_{21}-\eta_{03})^2+4\,\eta_{11}(\eta_{30}+\eta_{12})(\eta_{21}+\eta_{03})]$$

$$I_7 = (3\eta_{21}-\eta_{03})(\eta_{30}+\eta_{12})[(\eta_{30}+\eta_{12})^2-3(3\eta_{21}-\eta_{03})^2]+(\eta_{30}-3\,\eta_{12})(\eta_{21}+\eta_{03})[3(\eta_{30}+\eta_{12})^2 -(3\eta_{21}-\eta_{03})^2]$$

Table 8. I_2 Values of 30 Worms in Class 4 and its Mean & Variance

Serial Sample No. (Class 4)	I_2	Mean I_2	Variance
D1	0.0011	0.0016	2.34E-06
D2	0.0004		
D3	0.001		
D4	0.0026		
D5	0.0002		
D6	0		
D7	0.0008		
D8	0.0021		
D9	0.0013		
D10	0.0032		
D11	0.0046		
D12	0.0033		
D13	0.0001		
D14	0.0006		
D15	0.0022		
D16	0.0029		
D17	0.0026		
D18	0.002		
D19	0.0015		
D20	0.0014		
D21	0		
D22	0.0004		
D23	0.0004		
D24	0.006		
D25	0.0015		
D26	0.0002		
D27	0		
D28	0.0031		
D29	0.0036		
D30	0		

It can be seen from the table 8 that these moments do not vary much within the same class while it varies significantly from one class to another (which is later justified by F-test).

3.3 Statistical Analysis

The features extracted based on various methods require statistical evaluation for their test of significance. In fact, Fisher's F-test is used to obtain significant features out of many at certain level of significance. In this test, null hypothesis assumes equality of mean of each feature over all classes. Larger F value indicates rejection of null hypothesis i.e. feature is

statistically insignificant at β% level of significance. The formula for an F- test in multiple-comparison ANOVA problems is

$$F = \frac{\text{Mean square between samples}}{\text{Mean square within samples}}$$

4. Classification Using Error Backpropagation Neural Network

Neural networks are non-linear data modeling or decision making tools. They can be used to model complex relationships between inputs and outputs or to find patterns in data. Many algorithms of neural network have been proposed and been implemented as per their applications [12]. Feed forward backpropagation neural network is one of them and has been used for this work because it is simple, easy to train and has a good performance. Fig shows the architecture of the neural network for one hidden layer.

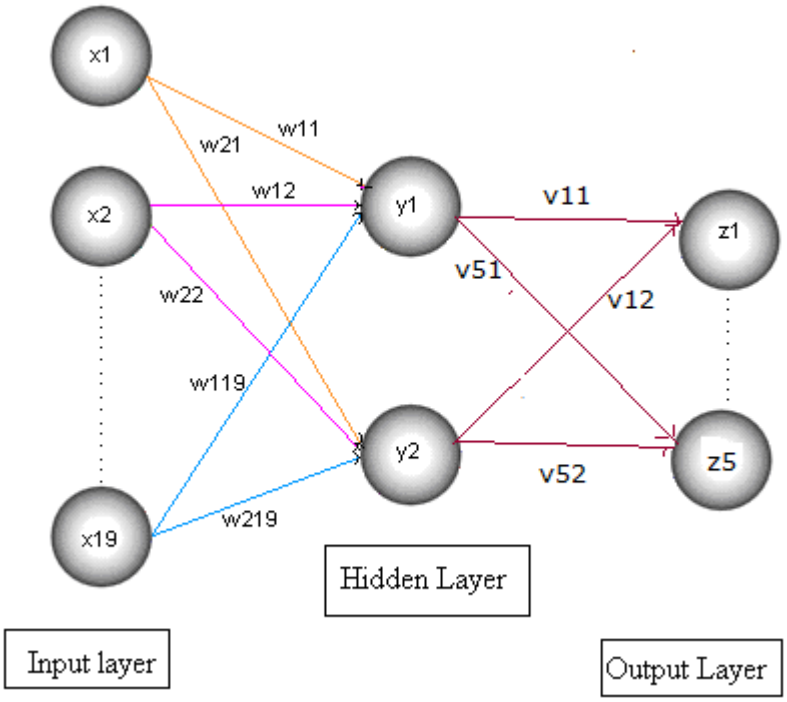

Figure 7. Neural Network Architecture for 19-2-5 Model

Backpropagation is the most widely used algorithm to train neural networks. The training is based on a simple concept: if the network gives a wrong answer, [13] then the weights are corrected so that the error is lessened and as a result, future responses of the network are more likely to be correct. It is an iterative algorithm where error gets propagated through the network from back and simultaneously is minimized using gradient descent optimization technique [12]. The minimization of error is done by adjustments to the weights. Firstly, the

derivatives of the error function with respect to the weights must be evaluated. Then the derivatives are used to compute the adjustment to be made to the weights. Furthermore/re, the weights are updated using the following rule:

$$\nabla w_{n+1} = \alpha \nabla w_n - \eta \frac{\partial E}{\partial w}$$

where ∇w_n and ∇w_{n+1} are the weight changes at epoch n and n+1, η is the learning rate, $\frac{\partial E}{\partial w}$ is the derivative of the error function with respect to the weights, and α is the momentum coefficient. The activation functions for hidden nodes and output nodes are non-linear function and mathematically it is sigmoid function and defined by

$$y(x) = \frac{1}{1 + e^{-\sigma x}}$$

where σ is constant and σ > 0. Error profile shows the error changing with each epoch. As the no. of epoch increases error decreases and finally it converges.

4.1 Sensitivity Analysis

Confusion matrix contains the information about actual and predicted classification. Performance of the system is described by the data of cell of the confusion matrix. Table shows the confusion for five class classifier. C_1, C_2, C_3, C_4, C_5 are the different classes and their entries in cell of the matrix have the following meaning. Suppose, a, g , m, e, s and y are the total no. of correct predictions and the rest of all are incorrect predictions. Then the matrix semantically can be presented as follows.

Table 9. Skeleton of the Confusion Matrix for 5 Classes

Confusion matrix		Actual				
		C_1	C_2	C_3	C_4	C_5
Predicted	C_1	a	b	c	d	e
	C_2	f	g	h	i	j
	C_3	k	l	m	n	o
	C_4	p	q	r	s	t
	C_5	u	v	w	x	y

Therefore, total accuracy of any system for *c* output class is given by

$$total \text{ accuracy} = \frac{1}{c} \sum_{i=1}^{c} \frac{\text{correctly classified for class i}}{\text{no of patterns in class i}}.$$

5. Results and Discussion

In this study, 150 worm images have been considered. From this image database all the features are computed and simultaneously evaluated for statistically significant using F test. As mentioned in Table 10 F-test shows I_5, I_6 and I_7 are not significant for significance level 1% .The descriptive statistics for these significant are shown in Table 11.

Table 10. Test of Significance of Worms' Shape Descriptors as Features

Features	F value	p value
I_5	1.634	0.169
I_6	3.726	0.006
I_7	0.055	0.995
others	6.22-548.5	0.000*

* $p<0.01$ indicates significant feature

Table 11. Summery Statistics for Significant Features

Features	Mean ± SD
Convexity	0.6549 ± 0.2294
Eccentricity	0.6625 ± 0.268
Compactness	0.0328 ± 0.026
I_1	0.7613 ± 0.8277
I_2	0.9889 ± 2.252
I_3	0.3373 ± 0.6715
I_4	0.086 ± 0.1623
Π_1	0.4704 ± 0.9688
Π_2	0.2046 ± 0.0233
Π_3	0.0219 ± 0.0143
Π_4	0.3312 ± 0.6575
Π_5	689.5527 ± 250.5553
Π_6	7070.463 ± 11030.16
Π_7	985.7841 ± 1742.36
Π_8	1.6155 ± 1.2927
Π_9	7.5085 ± 5.1776
Π_{10}	4.2743 ± 3.1789
Π_{11}	20.6677 ± 15.8058

Experimentally, the training set was taken to be 75% and the test set as 25% of the entire image database containing 150 patterns. The confusion matrix having the classification results of the network is presented in Table 12. This table shows that Balatidium coli and Ascaris are 100% correctly predicted, Fasciolopsis buski and tape worm are 71.14% correctly predicted while Aspergillus niger is 85.71% correctly predicted. Designing the architectures of the networks involves much trial and error, which is used to find the learning rate, and the momentum coefficient, etc. Here the optimum values of α and η are 1 and 0.8. Network has three layers architecture where the number of hidden units is chosen through the experimental performance. In this case, the hidden layer with 2 nodes performed best.

Table 12. Confusion Matrix

Confusion matrix		Actual no. of worm				
		Balatidium coli	Fasciolopsis buski	Aspergillus niger	Tape worm	Ascaris
Predicted no. of worm	Balatidium coli	8	1	0	0	0
	Fasciolopsis buski	0	5	1	0	0
	Aspergillus niger	0	0	6	0	0
	Tape worm	0	1	0	5	0
	Ascaris	0	0	0	2	8

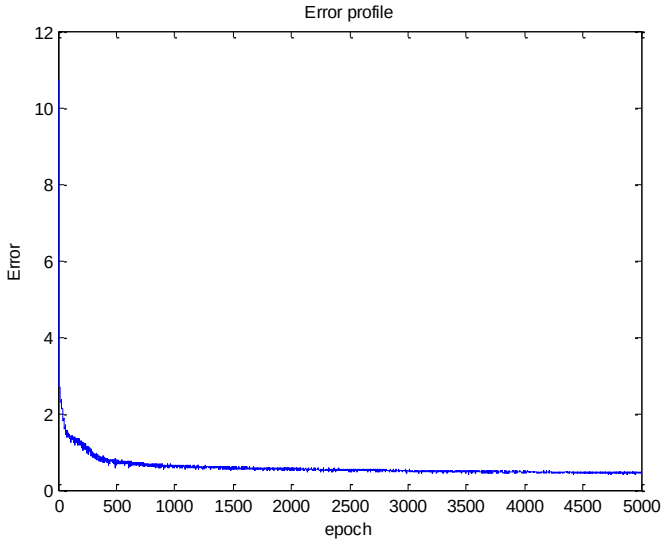

Figure 8. Error Profile for Backpropagation Neural Network

In addition, Figure 8 shows the error profile for each epoch of backpropagation neural network implemented using stochastic method. The error has been converged to 0.4678 at 2000 epoch.

6. Conclusions

Automatic classification of worm images from a huge central image database can be treated as one of the important application in biological domain. It can be observed that many of these parasites or fungi are responsible for human diseases. From diagnostic point of view, identification of these worms becomes more important. In order to quickly recognize specific worm class from standard database, a computer-aided classification system is developed with better understanding of the worms' shape descriptors. The system is more flexible as well as easier to implement. In this study, various region based shape descriptors, Hu's moments and other shape descriptors generated by trace transform, are used to represent an object. And finally, backpropagation neural network is trained and tested with 85.71% classification accuracy.

References

[1] S. K. Chang and A. Hsu, IEEE Trans, Knowledge Data Engg, vol. 5, no. 5, **(1992)**, pp. 431-442.
[2] H. Tamura and N.Yokoya, Pattern Recog., vol. 17, no. 1, **(1984)**, pp. 29-43.
[3] R. Duda, P. Hart and D. Stork, (Eds.), Pattern classification, Wiley, India, **(2007)**.
[4] N. Otsu, "A Threshold Selection Method from Gray-Level Histograms", IEEE Trans. Sys. Man. Cyber, vol. 9, no. 1, **(1979)**, pp. 62-66.
[5] R. C. Gonzalez and R.E. Woods, (Eds.), Digital Image Processing, Prentice Hall, **(2002)**.
[6] H. Samet, J. Assoc. Comp. Mach., vol. 28, no. 3, **(1981)**, pp. 487-501.
[7] A. T. Popov, Editor, "Fuzzy morphology and fuzzy convexity measures", Proceedings of the 13th Int'l Conf. on Pattern Recognition, **(1996)** August 25-29, Vienna, Austria.
[8] E. Rahtu, M. Salo and J. Heikkila, (Eds.), "Convexity Recognition Using Multi-Scale Auto convolution", Proceedings of the 17th Int. Conference on Pattern Recognition (ICPR'04), **(2004)** August 23-26; Washington, USA.
[9] A. Held and K. Abe, Pattern Recog. Lett., vol. 15, **(1994)**, pp. 611–618.
[10] A.Kadyrov and M. Petrou, IEEE Trans. Pattern Anal and Mach Intel., vol. 23, no. 8, **(2001)**, pp. 811-828.
[11] M. -K. Hu, IRE Trans. on Information Theory, IT-8, **(1962)**, pp. 179-187.
[12] C. M. Bishop, (Eds.), "Neural networks for pattern recognition", Oxford University Press, USA, **(1996)**.
[13] J. E. Dayhoff, (Eds.), "Neural network architectures - An introduction", International Thompson Publishing, USA, **(1990)**.